Interaction between antitumor drug and silver nanoparticles: combined fluorscence and surface enhanced Raman scattering study

Jing Yang (杨 晶)[1], Hong Wang (王 宏)[2], Zhuyuan Wang (王著元)[1], Xuebin Tan (谈学斌)[1], Chunyuan Song (宋春元)[1], Ruohu Zhang (张若虎)[1], Jin Li (李 锦)[1], and Yiping Cui (崔一平)[1*]

[1] *Advanced Photonics Center, Southeast University, Nanjing 210096, China*

[2] *Clinical Laboratory Center of the First Affliated Hospital of Nanjing Medical University, Nanjing 210006, China*

[*] *E-mail: cyp@seu.edu.cn*

Received July 14, 2009

Optical methods and MTT method are used to characterize the antiproliferation effect of antitumor drug 9-aminoacridine (9AA) with and without silver nanoparticles. Intracellular surface enhanced Raman scattering (SERS) spectra and fluorescent spectra of 9AA indicate the form of 9AA adsorbed on the surface of silver nanoparticles. Although both silver nanoparticles and antitumor drug can inhibit the growth of Hela cells, silver nanoparticles can slow down the antiproliferation effect on Hela cells at low concentration of antitumor drugs. Our experimental results suggest that silver nanoparticles may serve as slow-release drug carriers, which is important in antitumor drug delivery.

OCIS codes: 160.4236, 290.5860, 180.1790.

doi: 10.3788/COL20090710.0894.

In the field of drug therapy, materials of drug carriers are propitious to control the speed of drug to release in an effective range and last for a long time, in which case patients could suffer less from taking medicine for many times. Currently, drug delivery materials are focused on polymers micelle drug carriers[1], polysaccharides[2], proteins[3], peptides[4], lipids, and hydrogels[5,6], etc. Though great progress has been made on the design and synthesis of smart (stimuli-sensitive) drug carriers as well as the detection methods, there are few direct methods for monitoring the delivery process and providing spectra information in living biosystems. Instead, the physical and chemical properties of those drug carriers are usually measured before being applied to biosystems, or only the proliferation of the cells are observed to characterize the efficiency of the drug carriers.

Nanocarriers have been extensively investigated to facilitate the intracellular delivery of therapeutics[7,8]. Here, we use silver nanoparticles as the antitumor drug release materials. Compared with other drug release materials, the unique surface plasmonic properties of the silver particles make it possible to observe the drug release process in living cells by surface enhanced Raman scattering (SERS) method. As is well known, the usually weak Raman signals can be remarkably enhanced by several orders of magnitude when Raman scattering takes place on molecules at the surface or in the very close vicinity to noble metal nanostructures[9,10]. In recent years, SERS has become a promising tool for monitoring *in vitro* or *in vivo* biological processes[11−14]. The intercellular SERS signals provide direct information of the interactions between antitumor drug, silver nanoparticles, and living cells.

The antitumor drug 9-aminoacridine (9AA) is chosen as the drug model in the experiments. Acridine drugs are important intercalant molecules with mutagenic, antitumor, and antibacterial properties[15]. Up to now, 9AA has been successfully employed as antibacterial, mutagenic[16,17], and antitumor drug[18,19]. As an antitumor drug, 9AA exhibits antiproliferation effect on cancer cells. The acridine core intercalates DNA base pairs and then the formed drug-DNA complex blocks the activity of topoisomerase II, leading to a catalytic inhibition of the enzyme, an induction of apoptosis, and then a programmed cell death[20]. However, it is interesting that the antiproliferation effect of 9AA on Hela living cells can be slowed down at the presence of silver particles. We analyze such a phenomenon considering the intracellular interaction between 9AA and the surface of silver particles using combined SERS spectra and fluorescence spectra. Our experimental results suggest that silver nanoparticles may hold the potential for slow-release drug carriers.

Silver nanoparticles were synthesized by the method of Lee[21]. In brief, 18-mg $AgNO_3$ dissolved in 100-mL deionized water was heated to boiling. 2 ml of 1% trisodium citrate was added in the solution under intense stir. After 1-h boiling, the silver nanoparticles turned into gray color. The as-prepared colloid was stored in sealed and dark condition for future use.

Hela cells were purchased from Nanjing KeyGen Biotech Co., Ltd., and cultured in medium (DMEM) under a humidified atmosphere (5% CO_2 plus 95% air) at 37 °C. Media were supplemented with 10% heat-inactivated newborn calf serum (Hangzhou Every Green Organism Engineering Materials Co., Ltd.), and 1% penicillin-streptomycin. For fluorescence and SERS experiment, Hela cells were seeded into tissue culture dishes and incubated for 24 h. The culture medium was replaced by the one mixed with 9AA-adsorped silver nanoparticle dispersion (3:1 in volume ratio) and incubated for 7 h. For fluorescence images of the 9AA stained Hela cells, 10 μL of 1-mmol/L 9AA solution was added into the culture medium and incubated for 1 h.

Hela cells (10^4 /mL) were seeded onto 96-well plates (100 μL per hole) and incubated for 24 h at 37 °C under a 5% CO_2 atmosphere. Different concentrations of 9AA, 20-μL silver colloid, and the mixture of them were added to the medium and incubated for 14 h. The effects of 9AA, nanoparticles, and the mixture on cell proliferation were determined using the MTT (3-(4,5-dimethylthiazol-2-yl)-2,5-diphenyltetrazolium bromide) assay. 50 μL of MTT solution (MTT buffer to dilution buffer 1:4) was added to each well and the plates were incubated for 4 h. The reaction was terminated by adding 150 μL DMSO (Sigma) after removing the supernatant medium. When the purple formazan crystals were resolved by DMSO, the absorbance of the wells at 490 nm was measured with a microplate reader (BIO-RAD Model 680). Cells incubated in the absence of drugs and silver nanoparticles were used as controls. For each experiment, Hela cells were washed with phosphate buffered saline (PBS) for three times before use.

Absorption spectra were measured with a Shimadzu UV-3600 PC spectrophotometer. For absorption measurement of silver particles, 1-mL silver colloid was diluted to 3-mL with deionized water to prevent the saturation of absorption. For absorption measurement of the mixture of silver particles and 9AA, 1-mmol/L 9AA solution was added to 3 mL of the above diluted silver colloids with different volumes of 3, 5, 8, 10, 20, and 100 μL, respectively. Fluorescence spectra were obtained using Edinburgh FLS900 instruments. Intracellular fluorescence images were taken by an Olympus confocal scanning microscope. In the experiments, the excitation wavelength was selected at 458 nm. An oil immersion objective (60 ×) was used to focus the excitation beam. For SERS measurements, holographic notch filters were used to remove the Rayleigh scattering light and the Raman scatter light was directed to a spectrograph equipped with a Newton303i charge-coupled device (CCD) detector. A 10 × microscope objective was used to focus the excitation beam (argon ion laser, 514.5 nm with a power of 1.3 mW) to the sample surface.

As shown in Fig. 1, 9AA exhibits unique optical properties as having the symmetric ultraviolet (UV) absorption and fluorescent emission spectra. The spectrum of pure silver nanoparticles shows a single absorption peak at 420 nm due to the nanoparticle plasmon resonance, as shown in Fig. 2. The addition of 9AA to silver nanoparticles caused a significant decrease of the absorption peak while a new broad absorption band appeared at longer wavelength regions. The new band occurring in the near-infrared (NIR) region is well known to arise from the aggregation of nanoparticles formed upon the addition of the adsorbing molecules[22]. With the continuous addition of 9AA solution, the new absorption band exhibited a red shift with an intensity increase. The chloride ions of 9AA hydrochloride may induce the aggregation of silver nanoparticles which may result in large clusters. One thing needs to be mentioned is that a small band appeared and stacked on the band of silver colloid absorption spectrum when 10-μL 9AA solution was added into the silver colloid solution. It indicates that the 9AA molecules have already occupied all the surface sites by forming a monolayer. When more 9AA solution (12 μL) was added, a mountain-like absorption band belonging

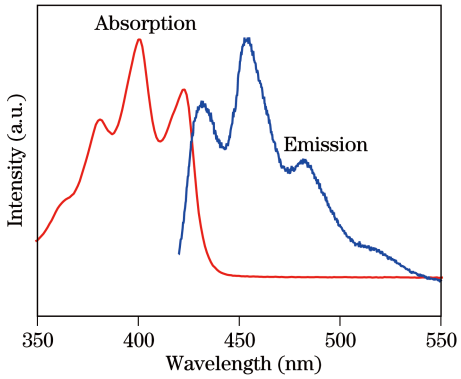

Fig. 1. Absorption and emission spectra of 9AA.

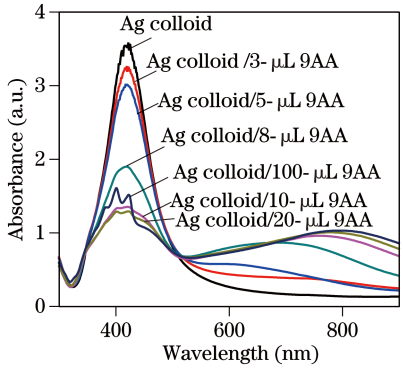

Fig. 2. Variation of absorption spectra as a function of the amount of 1-mmol/L 9AA added to 3-mL silver colloid nanoparticles (1-mL silver colloid was diluted to 3-mL with deionized water).

to 9AA absorption was obviously observed, indicating that the redundant 9AA molecules may have escaped from the silver surfaces. The concentration of 9AA at the turning point was 3.3 $\times 10^{-3}$ mmol/L.

To monitor the dynamic process of 9AA being added to the silver solution, fluorescence spectra were taken with different added amounts of 9AA. At the beginning, the fluorescence intensity of 9AA slowly increased linearly with the amount of added 9AA solution. In Fig. 3, it can be seen that when 10-μl 9AA solution was added, the fluorescence intensity increased suddenly and then increased linearly with the added 9AA amount. The above phenomena could be explained as follows. At the beginning, 9AA molecules continuously adsorbed onto the surface of silver nanoparticles. Since the fluorescences of most 9AA molecules were quenched due to the charge transfer to the metal surfaces, the fluorescence intensity of the whole mixture solution kept at a low level. Then with the further increase of the added amount of 9AA, they began to form a monolayer until the turning point was reached. Finally, after the surface sites of nanoparticles were occupied completely, the further added 9AA molecules started to dissociate into the mixture solution, and they were unable to be quenched by silver nanoparticles any more. That is to say, the dissociated molecules made a great contribution to the fluorescence intensity increase after the turning point. By curve fitting, the turning point was found to be 9.9 μL and the concentration of the 9AA was about 3.3 $\times 10^{-3}$ mmol/L. Thus, the fluorescence spectra measurement result proved a similar process of the interaction between 9AA molecules and

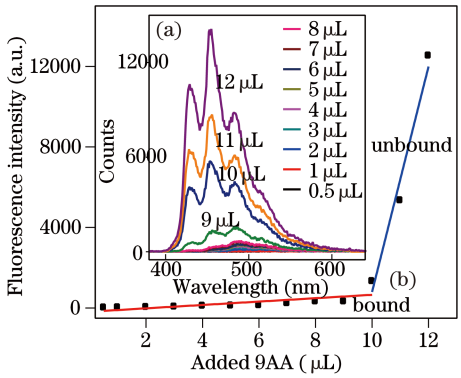

Fig. 3. Variation of fluorescence (a) spectra and (b) intensity.

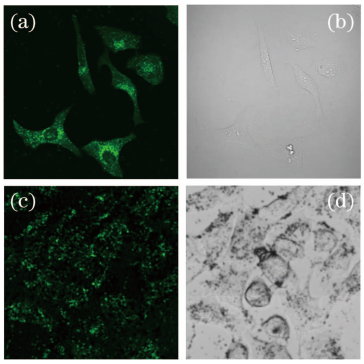

Fig. 4. (a) Fluorescence image of Hela cells labeled with 9AA, observed after 1 h of incubation; (b) transmission image of (a); (c) fluorescence image of Hela cells labeled with 9AA and silver nanoparticle complex, observed after 7 h of incubation; (d) transmission image of (c).

silver nanoparticles as compared with that obtained by absorption spectroscopy.

The intense fluorescence of 9AA makes it possible to detect its distribution in Hela cells by fluorescence images. As shown in Fig. 4, 9AA molecules were mainly located in the cytoplasm, especially in the endoplasmic reticulum. Only a fraction of 9AA molecules entered the cell nucleus. However, in the presence of silver nanoparticles, 9AA molecules were unable to have the same cellular distribution as in the pure 9AA stained cells. It could be deduced that when mixed with silver nanoparticles, some 9AA molecules could not move freely inside cells but adsorb on the surfaces of silver nanoparticles. More details are needed to explain how silver nanoparticles control the release of drugs inside the living cells.

For a better understanding of the 9AA releasing process in living cells at the presence of silver nanoparticles, intracellular 9AA SERS spectra were obtained and compared with those in solutions. Rivas *et at.* have reported that 9AA is adsorbed on the silver surface under two different forms: strongly attached 9AA characterized by imino form and weakly attached 9AA by amino form[23]. The obtained SERS spectra from 9AA incorporated in living Hela cells are shown in Fig. 5(b). Compared with the SERS spectra of 9AA in silver colloid solution, the SERS intensities of three bands decreased after 9AA being incorporated into living cells, the 1607-cm^{-1} band attributed to $\delta(NH_2)$ motions, 1560-cm^{-1}ring stretching vibrations coupled to exocyclic $\delta(NH_2)$ motions, and the 1255-cm^{-1} band contributed by γ(C-NH_2) vibrations. This demonstrated that the amino vibrations were weakened when the 9AA-absorbted silver nanoparticles entered into living Hela cells. To explain the SERS spectra changes of 9AA after being incorporated into living cells, two hypotheses are made. One is the change of pH environment, which will cause the tautomer form changes of 9AA molecules. The other is the decrease of the number of 9AA molecules with amino group. It is known that 9AA molecules adsorb to the silver surface through unprotonated imino form under alkaline and neutral pH condition, while through a protonated amino form under acid pH condition[24]. Considering that the pH value of the original prepared 9AA functionalized silver colloid is 10.04 but the pH environment of Hela cells is neutral except lysosomes (below 6), it could be deduced that the SERS decrease of amino band is not attributed to the change of pH value. So the decrease of amino vibration bands of intracellular SERS spectra could be due to the decrease of the amino formed 9AA molecules on the silver surfaces. That is to say, the spectral change of SERS spectra of 9AA under intracellular conditions may be caused by parts of the 9AA molecules breaking away from the surfaces of the silver nanoparticles due to the weakened bonding ability of amino groups. The escaping 9AA molecules may diffuse to the cytoplasm and exert the antitumor effect. All the above experimental results indicate that silver nanoparticles play an important role in controlling the drug release in biosystems.

As an antitumor drug, 9AA has a proliferation inhibition effect to Hela cells, and the survival rate decreases with the accumulated concentration of 9AA. As shown in Fig. 6, silver nanoparticles themselves can inhibit the cells at 89%. Besides, silver nanoparticles change the behaviors of the drug in living Hela cells. More interestingly, we find that the silver particles play different roles for the 9AA treated Hela cells when the 9AA concentration changes. For cells incubated with 9AA at high concentrations, silver nanoparticles increase the inhibition effect on proliferation. However, for those incubated with 9AA at low concentrations, silver nanoparticles reduce the inhibition effect on proliferation.

The fluorescence, absorption, and SERS spectra may give an answer to the above phenomenon. The interaction between 9AA molecules and silver nanoparticles plays a key role for the inhibition effect on proliferation of Hela cells at different 9AA concentrations. At low concentrations (below 3.3 $\times 10^{-3}$ mmol/L), 9AA molecules

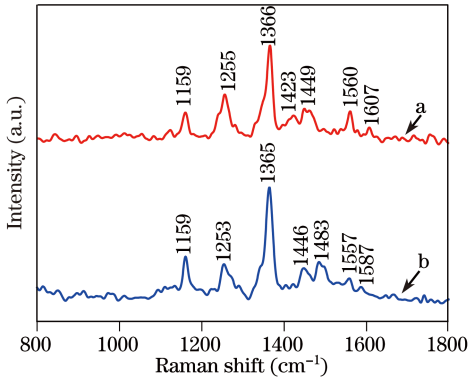

Fig. 5. SERS spectra of 9AA in (a) solution and (b) living Hela cells.

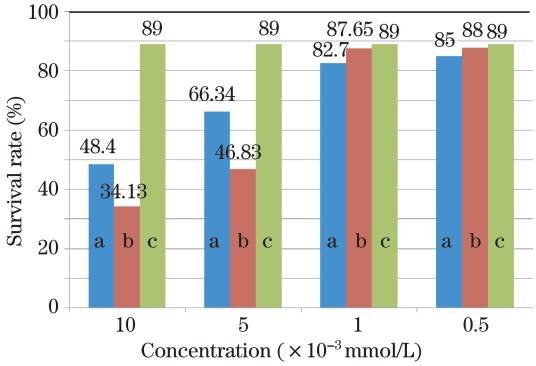

Fig. 6. Viability of Hela cells treated with different concentrations of 9AA and silver nanoparticles. (a) Pure 9AA; (b) 9AA and silver nanoparticle complex; (c) pure silver nanoparticles.

is not enough to occupy all the surface sites. The interaction between 9AA molecules and silver particles is so strong that most of the 9AA molecules with imino groups are unable to escape from the surfaces of silver nanoparticles. So the adsorbed imino formed 9AA molecules cannot exert the drug effect as much as those in free. As a result, the survival rate of the cells is higher than those incubated with pure 9AA at the same concentration. On the contrary, in the case of cells incubated with 9AA at high concentrations (above 3.3 $\times 10^{-3}$ mmol/L), 9AA molecules keep adsorbing on the surfaces of silver nanoparticles until a monolayer is formed. The redundant 9AA molecules and the adsorbed 9AA molecules through amino groups will escape from the silver surfaces and diffuse to the cytoplasm, leading to an increased inhibition effect on proliferation. Besides, a high concentration of 9AA will induce the silver nanoparticles to form large aggregations having a great injury to the cellular membrane, which may also contribute to the increased inhibition on the proliferation at high 9AA concentration. So the survival rate of Hela cells treated with the silver and 9AA complex at high 9AA concentrations is lower than those incubated with pure 9AA at the same concentration.

In conclusion, we have investigated the intracellular interaction between antitumor drug 9AA and silver nanoparticles using the combined SERS spectra and fluorescence spectra. We have observed different antiproliferation effects of 9AA on Hela cells with and without silver nanoparticles. It is found that silver nanoparticles can be used to control the release of 9AA in living cells. The reason may be that silver nanoparticles can hold the surrounding 9AA molecules to its surface until a monolayer is formed. The way 9AA adsorbing on the silver surfaces plays an important role in their delivery effect in living cells. Compared with other drug release methods such as using polymers or silica nanoparticles, the way using silver nanoparticles has the advantage of providing more spectral information, such as SERS spectra. By optimizing the surface modification, silver nanoparticles may hold great potential in smart drug carrier applications.

This work was supported by the National Natural Science Foundation of China (Nos. 60708024 and 60877024).

References

1. Y. Bae, W. D. Jang, N. Nishiyama, S. Fukushima, and K. Kataoka, Mol. Biosyst. **1,** 242 (2005).
2. G. Berth, A. Voigt, H. Dautzenberg, E. Donath, and H. Möhwald, Biomacromolecules **3,** 579 (2002).
3. Z. L. Zhi and D. T. Haynie, Chem. Commun. **2,** 147 (2006).
4. D. T. Haynie, N. Palath, Y. Liu, B. Y. Li, and N. Pargaonkar, Langmuir **21,** 1136 (2005).
5. M. Ehrbar, R. Schoenmakers, E. H. Christen, M. Fussenegger, and W. Weber, Nature Mater. **7,** 800 (2008).
6. H. W. Tang, X. R. Duan, X. L. Feng, L. B. Liu, S. Wang, Y. L. Li, and D. B. Zhu, Chem. Commun. **6,** 641 (2009).
7. S. V. Vinogradov, T. K. Bronich, and A. V. Kabanov, Adv. Drug Deliv. Rev. **54,** 135 (2002).
8. G. S. Kwon, Crit. Rev. Ther. Drug Carrier Syst. **20,** 357 (2003).
9. M. Fleischman, P. J. Hendra, and A. J. McQuillan, Chem. Phys. Lett. **26,** 163 (1974).
10. D. L. Jeanmaire and R. P. Van Duyne, J. Electroanal. Chem. **84,** 1 (1977).
11. J. Kneipp, H. Kneipp, B. Wittig, and K. Kneipp, Nano Lett. **7,** 2819 (2007).
12. C. E. Talley, L. Jusinski, C. W. Hollars, S. M. Lane, and T. Huser, Anal. Chem. **76,** 7064 (2004).
13. K. N. Yu, S. M. Lee, J. Y. Han, H. Park, M. A. Woo, M. S. Noh, S. K. Hwang, J. T. Kwon, H. Jin, Y. K. Kim, P. J. Hergenrother, D. H. Jeong, Y. S. Lee, and M. H. Cho, Bioconjugate Chem. **18,** 1155 (2007).
14. X. M. Qian, X. H. Peng, D. O. Ansari, Q. Yin-Goen, G. Z. Chen, D. M. Shin, L. Yang, A. N. Young, M. D. Wang, and S. M. Nie, Nature Biotechnol. **26,** 83 (2008).
15. A. Murza, S. Sánchez-Cortés, and J. V. García-Ramos, Biopolymers. **62,** 85 (2001).
16. H. P. Zhu, S. M. Clark, S. C. Benson, H. S. Rye, A. N. Glazer, and R. A. Mathies, Anal. Chem. **66,** 1941 (1994).
17. C. Rehn and U. Pindur, Monatsh. Chem. **127,** 645 (1996).
18. E. L. Loechler and J. King, Biochemistry **25,** 5858 (1986).
19. D. Fornasiero and T. Kurucsev, Biophys. Chem. **23,** 31 (1985).
20. J. R. Goodell, A. V. Ougolkov, H. Hiasa, H. Kaur, R. Remmel, D. D. Billadeau, and D. M. Ferguson, J. Med. Chem. **51,** 179 (2008).
21. P. C. Lee and D. J. Meisel, J. Phys. Chem. **86,** 3391 (1982).
22. C. G. Blatchford, J. R. Campbell, and J. A. Creighton, Surf. Sci. **120,** 435 (1982).
23. L. Rivas, A. Murza, S. Sánchez-Cortés, and J. V. García-Ramos, Vibrational Spectroscopy **25,** 19 (2001).
24. A. Murza, S. Sánchez-Cortés, and J. V. García-Ramos, Biospectroscopy **4,** 327 (1998)
25. J. Rak, P. Skurski, M. Gutowski, L. Jozwiak, and J. Blazejowski, J. Phys. Chem. A **101,** 283 (1997).